Chemistry and Physics of Lipids 225 (2019) 104811

Contents lists available at ScienceDirect

Chemistry and Physics of Lipids

journal homepage: www.elsevier.com/locate/chemphyslip

Study of release kinetics and degradation thermodynamics of ferric citrate liposomes

Shan Wang, Wenxin Li, Kaiyue Sun, Ru Zhang, Shuping Wang, Lina Geng*

College of Chemistry and Material Science, Hebei Normal University, Shijiazhuang, 050024, China

ARTICLE INFO

Keywords:
Ferric citrate liposome
In vitro release
Release kinetics
Degradation thermodynamics

ABSTRACT

Ferric citrate liposome (FAC-Lip) with good sustained-released property was prepared by the rotary-evaporated film-ultrasonic method, and characterized by TEM, DLS, zeta potential and encapsulation efficiency (EE%). The effects of membrane material ratios (m_{PC}: m_{chol} = 8:1, 10:1 and 12:1) and drug lipid ratios (m_{FAC}: m_{PC} = 1:4, 1:6.5 and 1:8) on the release of FAC-Lip were examined. The *in vitro* release kinetic models and mechanisms of FAC-Lip in artificial gastric juice (SGF) and artificial intestinal juice (SIF) compared with free-FAC were determined. The thermal degradation in PBS was also determined. The results showed that FAC-Lip with membrane material ratio (10:1) and drug lipid ratio (1:6.5) had the optimal sustained-released property, unilamellar vesicles with uniform size (178 ± 2.12 nm), negative charge (−56 ± 3.51 mV) and high encapsulation efficiency (72.77 ± 0.42%). The *in vitro* release kinetic models of FAC-Lip were two-phase kinetics model and the release mechanisms were non-Fick diffusion both in SGF and SIF. The thermal degradation of FAC-Lip was an endothermic and spontaneous reaction. The results may be helpful in optimizing drug-liposome design, application in food and medicine industries, and furthermore, predicting and guiding medication *in vivo*.

1. Introduction

Iron is one of the essential trace elements in the human body and plays an important role in the body's activities and metabolism. (Jonker and Boele van Hensbroek, 2014) Iron deficiency can lead to iron deficiency anemia (IDA). At present, there are more than two billion people suffering from IDA in the world. The World Health Organization has listed IDA as one of the major nutritional diseases in the world. (Lopez et al., 2016) IDA is usually caused by insufficient intake of iron-containing food or excessive iron consumption (Gupta et al., 2015). Currently, oral iron supplement or increasing iron content in food is the best way to prevent iron deficiency (Powers and Buchanan, 2014). The common iron supplement agent is small molecular organic iron salt, represented by ferric citrate (FAC), which has the disadvantages of poor taste, poor stability and low bioavailability (McCullough et al., 2018). Liposomes are artificial bilayer membranes with non-toxic and non-immunogenic properties and can be used as a carrier for drugs (Eloy et al., 2014). Liposomes can be easily absorbed and degraded *in vivo* due to having a similar structure to that of cellular membranes, and their encapsulation also can reduce drug consumption, improve absorption efficiency and lower toxicity. (Huang et al., 2016)

In recent years, researchers have been working to study the stability of drug-loaded liposomes by studying related parameters, such as release kinetics and degradation thermodynamics *in vitro*. The common experiments *in vitro* release are to simulate the physiological environment *in vivo*, such as the artificial gastric juice (SGF) and artificial intestinal juice (SIF). (Hu et al., 2013) The data of *in vitro* release can be used to predict the drug release *in vivo*, that contributes to understand the biopharmaceutical characteristics of the formulation and provides a basis for preparing a better sustained release formulation. (Preiss et al., 2017) The optimal conditions of sustained release of ferric citrate liposome (FAC-Lip) have rarely been investigated. Particularly, the effects of membrane material ratios and drug lipid ratios *in vitro* release of FAC-Lip have not been investigated.

In order to further study the *in vitro* release behaviors of drugs, researchers have been working on fitting the drug release data with some kinetic models to judge the drug release models and mechanisms. Common release kinetic models include zero-order kinetic model, first-order kinetic model, Weibull model, Higuchi model, Ritger-Peppas model and two-phase kinetic model. (Jain and Jain, 2016) Ho Yub Yoona et al. demonstrated that the *in vitro* release of docetaxel liposomes belonged to first-order equation. (Yoon et al., 2017) Ajda Ota et al. have reported that alginate microparticles and alginate microparticles loaded with liposomes followed Higuchi model, which suggested that pantothenic acid release was mainly driven by a diffusion controlled mechanism (Ota et al., 2018). M. Quilaqueo et al. confirmed

* Corresponding author.
E-mail address: genglina0102@126.com (L. Geng).

https://doi.org/10.1016/j.chemphyslip.2019.104811
Received 27 March 2019; Received in revised form 10 June 2019; Accepted 16 August 2019
Available online 23 August 2019

that the released mechanism of quercetin liposome was agreed with Fick diffusion, whereas the release mechanism of rutin liposome was agreed with non-Fick diffusion (Silva-Weiss et al., 2018). In current, the kinetic model and release mechanism of FAC-Lip have not been studied.

Moreover, degradation is one of the important factors to evaluate drug-liposome stability, and also the main basis for determining the validity period and storage condition. (Hirai et al., 2015) FAC-Lip is a thermodynamically unstable system in which the particles are easy to aggregate during storage, resulting in a larger size. Meanwhile, the phospholipids contain unsaturated bonds, which are prone to hydrolysis and oxidation, (He et al., 2000) resulting in drugs leakage and degradation, which seriously limited its application in pharmaceuticals and foods. Currently, researchers have obtained the related parameters such as degradation rate constant (k), activation energy (E_a), Gibbs free energy change (ΔG), enthalpy change (ΔH) and entropy change (ΔS) and degradation models through the thermodynamics and kinetics data of degradation, and the effect of temperature on degradation. Alejandra I. Pérez-Molina et al. reported that the ΔG of laminarinase in soya lecithin liposomes at 25 ℃ was negative, which confirmed that laminarinase transfer from aqueous media to an organic system was spontaneous and the ΔH of laminarinase was positive, which confirmed that the process was endothermic. (Pérez-Molina et al., 2011) Xiaoyong Wang et al. demonstrated that the release of curcumin liposomes followed first order kinetic model (Niu et al., 2012). Chunyong Wu et al. confirmed that the E_a of cabozantinib was 57.31 kJ/mol, which represented the moderate sensitivity of the degradation process to temperature in the range of 50–96 kJ/mol. (Wu et al., 2014) The effect of temperature on the degradation of FAC-Lip has rarely been investigated, and the thermodynamic parameters have also not been investigated.

In previous work, we investigated the interaction between the drug and the phospholipid membrane in FAC-Lip, mainly electrostatic interaction and hydrogen bonding, and calculated the ΔG between drug and liposome membrane. (Li et al., 2015) The influence of drug molecular weight, structure, membrane interaction, and particle size of liposomes on drug release had also been discussed (Guo et al., 2017). We also examined the therapeutic effect of FAC-Lip on anemia model mice, the results showed that the ferric citrate encapsulated by liposome could effectively increase the available iron content in the body and significantly alleviate the symptoms of anemia. (Yuan et al., 2013)

In this study, we designed to prepare FAC-Lip with good sustained release property by the rotary-evaporated film-ultrasonic method. We explored the optimal ratios of sustained release property by studying the effects of membrane material ratios and drug lipid ratios on release of FAC-Lip *in vitro*. The physicochemical properties of the optimal conditions of FAC-Lip were evaluated by measuring encapsulation efficiency, morphology, particle sizes and zeta potential. In addition, we used six classical release kinetic models to study the release of FAC-Lip compared with free-FAC in SGF and SIF. We also explored the effect of temperature on the degradation of FAC-Lip and analyzed the thermodynamic parameters, such as E_a, ΔH, ΔG and ΔS.

2. Materials and methods

2.1. Materials

Materials were used as obtained from commercial sources unless otherwise noted. Ferric citrate (FAC, Grade: USP) was purchased from Sigma-Aldrich (St. Louis, MO, USA). Soybean lecithin (> 75%) was provided by Yuan Hua Mei Lecithin Sci-Tech Co., Ltd. (Beijing, China). Cholesterol (Chol, > 95%) and dialysis bag (MWCO 3500) were obtained from Yuanye Bio-Technology Co., Ltd (Shanghai, China). All other chemicals and solvents used were of analytical grade, offered by Bodi Chemical Co., Ltd. (Tianjin, China).

2.2. Preparation of FAC-Lip

FAC-Lip was prepared by the rotary-evaporated film-ultrasonic method. (Li et al., 2017) Cholesterol and lecithin (m_{PC}: m_{chol} = 8:1, 10:1 and 12:1) were dissolved in an ethanol solution. The organic solvent was removed by evaporation in a rotary evaporator at 45 ˚C under vacuum over 30 min. When the thin film was formed, hydrated with FAC (m_{FAC}: m_{PC} = 1:4, 1:6.5 and 1:8, respectively, dissolved in phosphate-buffered saline (PBS), pH = 6.5) and glass beads (3–4 mm diameter) were added. The mixture was rotated for 40 min until the lipid film was hydrated and formed a suspension. The suspension was dispersed by ultrasonication for 20 min (100 W), and then dialyzed (MWCO 3500), and the dialysate was changed every 6 h until the amount of FAC was not detectable in the dialysate. The FAC-Lip was stored in a brown bottle at 4 ℃. Based on the good sustained release property of FAC-Lip, the optimum ratio of membrane material ratios and drug lipid ratios were determined.

2.3. In vitro drug release study

Artificial gastric juice and artificial intestinal juice were prepared according to the methods described in Chinese Pharmacopoeia. (Hu et al., 2013) Artificial gastric juice (SGF) was prepared as follows: 3 mL HCl diluted solution, 100 mg NaCl and 160 mg pepsin were added to 50 mL deionized water and mixed. Finally, the pH was adjusted to 1.3. Artificial intestinal juice (SIF) was prepared as follows: 76 mg NaOH, 340 mg KH_2PO_4 and 500 mg trypsin were added to 50 mL deionized water and mixed, Finally, the pH was adjusted to 7.5.

The *in vitro* release of FAC-Lip and free-FAC in artificial gastric juice (SGF) and artificial intestinal juice (SIF) were determined using dialysis diffusion technique, and explored the optimal sustained release ratios. (Mahobia et al., 2018) In brief, 2 mL of FAC-Lip suspension (membrane material ratios were 8:1, 10:1 and 12:1, drug lipid ratios were 1:4, 1:6.5 and 1:8) was transferred to a dialysis bag (MWCO 3500), and then immersed in 80 mL release medium, that was incubated at 37 ˚C and shook at 60 rpm with protecting from light. At scheduled time intervals (0, 0.5, 1, 2, 4, 6, 8, 10, 12, 15, 18, 21, 24, 28, 32 h, *etc.)*, 1 mL solution was taken from the dialysate and replaced with fresh medium to maintain a constant volume (Machado et al., 2018). The release of free-FAC in the same buffer was also tested for comparison. The release amount of FAC was determined at 260 nm using ultraviolet spectrophotometry (U3010, Hitachi, Japan), from which the cumulative drug release *versus*of FAC-Lip was calculated using the following formula: (Yuan et al., 2013; Gibis et al., 2016)

$$\text{Cumulative drug release versus (Q\%)} = \frac{M_t}{M_T} \times 100\% \quad (1)$$

where, M_t represents the mass of FAC encapsulated in the dialysate at t hours post-incubation, and M_T represents the mass of FAC encapsulated in the liposomes before incubation.

2.4. Characterization of FAC-Lip

Morphology of FAC-Lip was analyzed by transmission electron microscope (TEM). For TEM observation, FAC-Lip was diluted with distilled water and a drop of it was placed on a copper grid and was allowed to adsorb. Further this was stained using a drop of 4% (w/v) solution of phosphotungstic acid for 30 s. The excess solution was removed by blotting with filter paper and the sample was allowed to dry at room conditions. Images were captured using a JEM-100SX TEM (Hitachi, Japan).

The size and zeta potential of FAC-Lip were determined using dynamic light scattering (DLS) with Nano-ZS (Malvern Instruments Ltd, Malvern, UK). The sample was diluted with ultrapure water. All measurements were carried out at room temperature.

The encapsulation efficiency of FAC-Lip was calculated using our

previous method and the following equation: (Lu et al., 2011)

$$\text{Encapsulation Efficiency (EE \%)} = 1 - \frac{m_t}{m_T} \times 100\% \quad (2)$$

where, m_T is the total amount of FAC initially addition and m_t is the amount of FAC in the liposome.

2.5. Kinetic models and mechanisms of in vitro release

Six classical release kinetic models were used to study the release models and mechanisms of FAC-Lip in SGF and SIF. Zero order kinetic models can be represented mathematically as:

$$Q = k_0 t + A \quad (3)$$

where, Q is the amount of drug released, A is the initial amount of drug in solution (it is usually zero), and k_0 is the zero order release rate constant. This release kinetics can be used for transdermal drug delivery, ophthalmic drug delivery and low water solubility drug delivery. (Nayak and Malakar, 2011) First order kinetic model was given by Noyes and the integrated form is given as:

$$Q = A(1 - \exp(-k_1 t)) \quad (4)$$

where, Q is the amount of drug released, and k_1 is first order release rate constant. First order kinetics model describes mainly the mechanism of dissolution in pharmaceutical dosage forms as water soluble drug in porous matrices. Weibull model has the form of a stretched exponential and used in drug release studies as well as in dissolution studies and the integrated form is given as:

$$Q = A(1 - \exp(-(k_w(t - tb))^c) \quad (5)$$

where, k_W is the release rate constant, and b is constants. This functional form is derived as an approximation in the framework of fractal kinetics (Papadopoulou et al., 2006). Higuchi model explains the release of drug through an insoluble matrix based on Fick diffusion model which is given as:

$$Q = k_H t^{0.5} + A \quad (6)$$

where, k_H is the Higuchi dissolution constant, *i.e.*the release rate constant for the Higuchi model. (Siepmann and Peppas, 2001) Ritger-Peppas model gives simple relationship about diffusion related to the drug release from a polymeric system. This model is mathematically represented as:

$$Q = k_P t^n \quad (7)$$

where, Q is the amount of drug released, and k_P is the release rate constant and n is the release exponent. (Dash et al., 2010) Two-phase kinetic model reflected that the percutaneous penetration of the drug is an exponential attenuation model and the integrated form is given as:

$$Q = 1 + A\exp(ct) + B\exp(dt) \quad (8)$$

where, Q is the amount of drug released, c and d are two release rate constants of the formulation, respectively. (Beltran Osuna and BoyacaMendivelso, 2010)

2.6. Release mechanism

The release mechanism was analyzed by Ritger-Peppas equation ($Q = k_P t^n$). The value of n is the release index indicating the drug release mechanism, $n < 0.45$ corresponds to Fick diffusion mechanism, $0.89 \geq n \geq 0.45$ to non-Fick diffusion (drug diffusion and matrix dissolution), $n > 0.89$ to case II transport (skeleton dissolution). (Silva-Weiss et al., 2018; Koutsoulas et al., 2014)

2.7. The thermal degradation of FAC-Lip

The thermal degradation of FAC-Lip was investigated in PBS (pH = 6.5) in the dark for 72 h at different temperatures (277, 298 or 310 K). The residual rate of FAC was calculated according to Eq. (9). (Yang et al., 2018) In brief, took 0.5 mL FAC-Lip and 2 mL xylene were added into a centrifuge tube for demulsification, centrifuged at 3500 *g*for 20 min, and then centrifuged at 4000 *g*for 10 min. The supernatant was taken, diluted and measured the absorbance at A_{260}. The degradation of free-FAC in the same buffer was also tested for comparison.

$$\text{Residual rate (\%)} = \frac{C_t}{C_T} \times 100\% \quad (9)$$

where, C_t is the residual FAC mass concentration (mg/mL) at t time, and C_T is the initial addition of FAC mass concentration (mg/mL).

2.8. Thermodynamic parameters

The thermodynamic parameters of FAC-Lip were studied, including the activation energy (E_a), Gibbs free energy change (ΔG), enthalpy change (ΔH) and entropy change (ΔS). E_a, ΔG, ΔH and ΔS were calculated using the Arrhenius and Eyring equation:

$$\ln k = \ln K_0 - \frac{E_a}{RT} \quad (10)$$

$$\Delta H = E_a - RT \quad (11)$$

$$\Delta G = -RT\ln\left(\frac{hk}{k_B T}\right) \quad (12)$$

$$\Delta S = \frac{(\Delta H - \Delta G)}{T} \quad (13)$$

where, E_a is the activation energy (kJ/mol), R is the gas constant ($(8.314\ J{\cdot}mol^{-1}K^{-1}$-$^{-1}K^{-1})8.314\ J{\cdot}mol^{-1}K^{-1}$), T is the absolute temperature (K), k_B is Boltzmann constant (1.3806×10^{-23}J/K), h is the Planck constant (6.6262×10^{-34} JJ/s), ΔH is the enthalpy change at each temperature (kJ/mol), ΔG is the Gibbs free energy change (kJ/mol), and ΔS is the entropy change ($J{\cdot}mol^{-1}{\cdot}K^{-1}$) (Pérez-Molina et al., 2011; Rupar et al., 2018)

2.9. Statistical analysis

The data was fitted using Origin 8.0 software. All experiments were performed at least in triplicate.

3. Results and discussion

3.1. The sustained-released properties

The sustained-released property of FAC-Lip with different membrane material ratios (m_{PC}: m_{chol} = 8:1, 10:1 and 12:1) and drug lipid ratios (m_{FAC}:m_{PC} = 1:4, 1:6.5 and 1:8) was detected (Fig. 1). As shown in Fig. 1a, the three FAC-Lip with different membrane material ratios had sustained-released effect, and the maximum cumulative release amount exceeded 90%. The release rates of the three FAC-Lip were fast at the first 6 h, and then gradually slowed down with the continuous reduction of the concentration difference between the inside and outside of the dialysis bag, without sudden release. However, with the increase of membrane material ratio, the sustained release effect of FAC-Lip increased first and then decreased, so it was considered that the best membrane material ratio of FAC-Lip was 10:1.

Fig. 1b schematically showed the cumulative release profile of FAC from FAC-Lip with different drug lipid ratios. The release rates of the three FAC-Lip were fast during the first 6 h, and then gradually slowed down and no sudden release occurred. By contrast, FAC-Lip with drug lipid ratio 1: 6.5 had the optimal sustained release property. According the sustained-released property, the optimization proportions were selected (m_{PC}: m_{chol} = 10: 1 and m_{FAC}: m_{PC} = 1: 6.5).

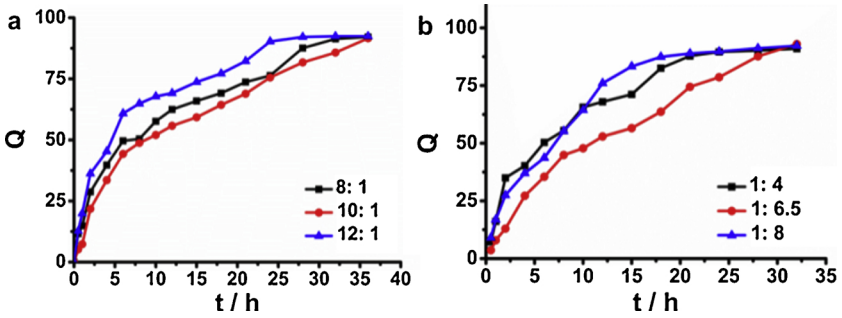

Fig. 1. *In vitro* release of FAC-Lip with different membrane material radios (8: 1, 10: 1 and 12: 1) (a) and drug lipid ratios (1:4, 1:6.5 and 1:8) (b).

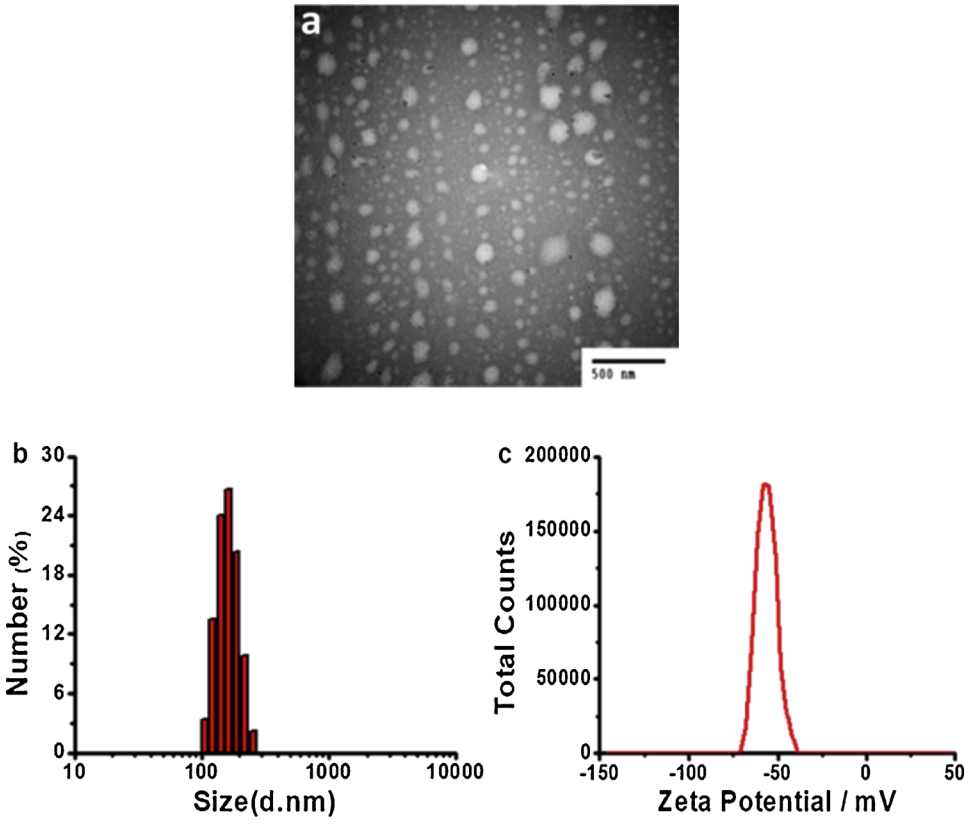

Fig. 2. TEM image (a), particle size distribution (b) and zeta potential (c) of FAC-Lip.

3.2. Characterization of FAC-LIP

FAC-Lip was produced using standard thin film hydration and sonication method, and the physicochemical properties of FAC-Lip with optimal sustained release ratio were evaluated by TEM, DLS, zeta potentials and encapsulation efficiency(EE%).

The microstructure of FAC-Lip was observed by TEM image (Fig. 2a). It showed well-formed spherical and the size range was about 100–200 nm. DLS showed the size distribution of FAC-Lip and the average particle size was approximately 178 ± 2.12 nm (Fig. 2b). As a carrier system, the size of liposomes had significant influence on the efficacy *in vivo* (Limasale et al., 2015). Small particle sizes (< 200 nm) could ensure to increase vascular permeability, lower level of reticuloendothelial system uptake, and improve utilization ratio of entrapped compound. (Soni et al., 2008). Therefore, the size range of FAC-Lip prepared was appropriate for *in vivo* delivery in this study.

The zeta potential charge is an important characteristic determining liposome stability. It reflects the function of the lipid charge or any adsorbed layer at the interface and the nature and composition of the medium in which the liposomes are suspended. (Allison et al., 2007) In general, liposomes are stable when the absolute value of the zeta potential is greater than 30 mV, as their charge inhibits coalescence and enhances stability (Kandzija and Khutoryanskiy, 2017). In our study, the zeta potentials of FAC-Lip were about −56 ± 3.51 mV (Fig. 2c), reflecting the high physical stability.

Encapsulation efficiency is a critical parameter in drug delivery system. The ability to encapsulate a sufficient amount of therapeutic agent is one of the most desirable properties for liposomes. In our experiment, FAC-Lip (m_{PC}: m_{chol} = 10: 1 and m_{FAC}:m_{PC} = 1: 6.5) had high encapsulation efficiency, about 72.77 ± 0.42%.

3.3. Kinetic models and mechanisms of release of FAC-Lip in SGF and SIF

The release of FAC-Lip and free-FAC in SGF and SIF were shown in Fig. 3, respectively, demonstrating that both FAC-Lip and free-FAC could release 90% in SGF and SIF. Fig. 3a showed that free-FAC released more than 90% at about 20 h in SGF, while the release of FAC-Lip reached equilibrium at about 140 h; Fig. 3b showed that free-FAC released completely in SIF at about 15 h, while FAC-Lip at about 25 h. It indicated that FAC-Lip has a significant sustained release capacity

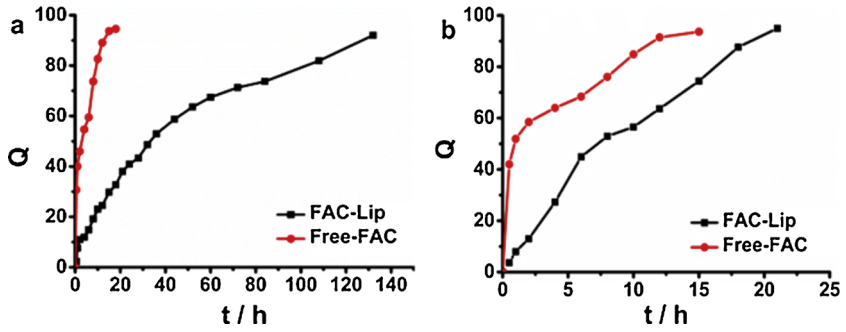

Fig. 3. Release curves of FAC-Lip and free-FAC in SGF (a) and SIF (b).

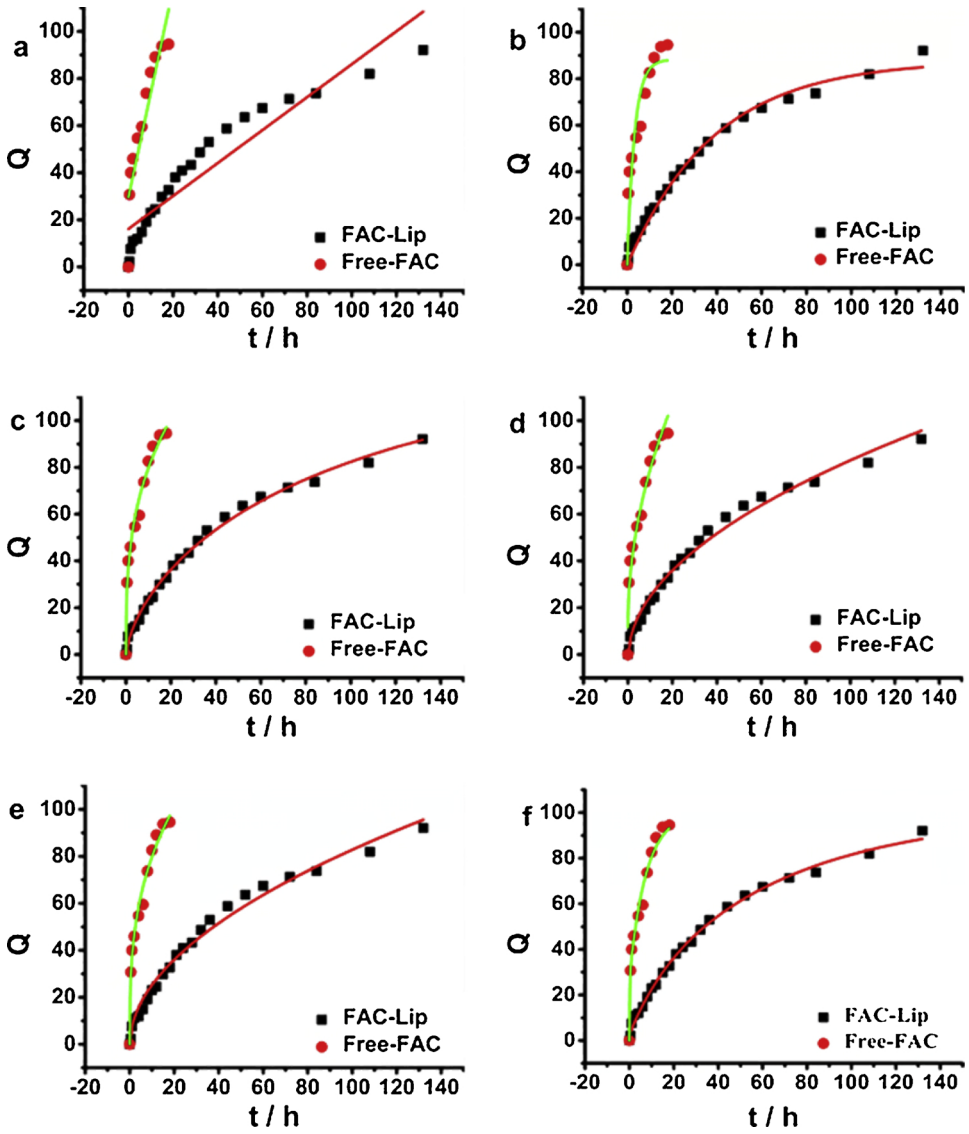

Fig. 4. Release curves of FAC-Lip and free-FAC simulated with Zero order kinetic model(a), First order kinetic model (b), Weibull model (c), Higuchi model (d), Ritger-Peppas model (e), two-phase kinetic model (f) in SGF.

compared to free-FAC. Generally, the gastric emptying time was usually 2–3 hours. (Shen et al., 2014) The amount of drug released from FAC-Lip was very little during this period, indicating that the gastric environment has less effect on the stability of FAC-Lip and allows more drugs to reach the intestinal tract, greatly improving the oral bioavailability of FAC-Lip.These characteristics were consistent with our design goal, that was, the more absorption of FAC-Lip in the intestine and less loss in gastric juice.

3.4. Release kinetic models

In order to further study the release of FAC-Lip and free-FAC in the two above medias, the release curves were fitted by Eq. (3)–(8) (Fig. 4 and 5). According to the fitting coefficient (R^2), the best model was determined, and the fitting results were shown in Table 1 and 2.

As can be seen from Table 1, the maximum R^2 of FAC-Lip was 0.9955, so the release of FAC-Lip in SGF was consistent with two-phase kinetic

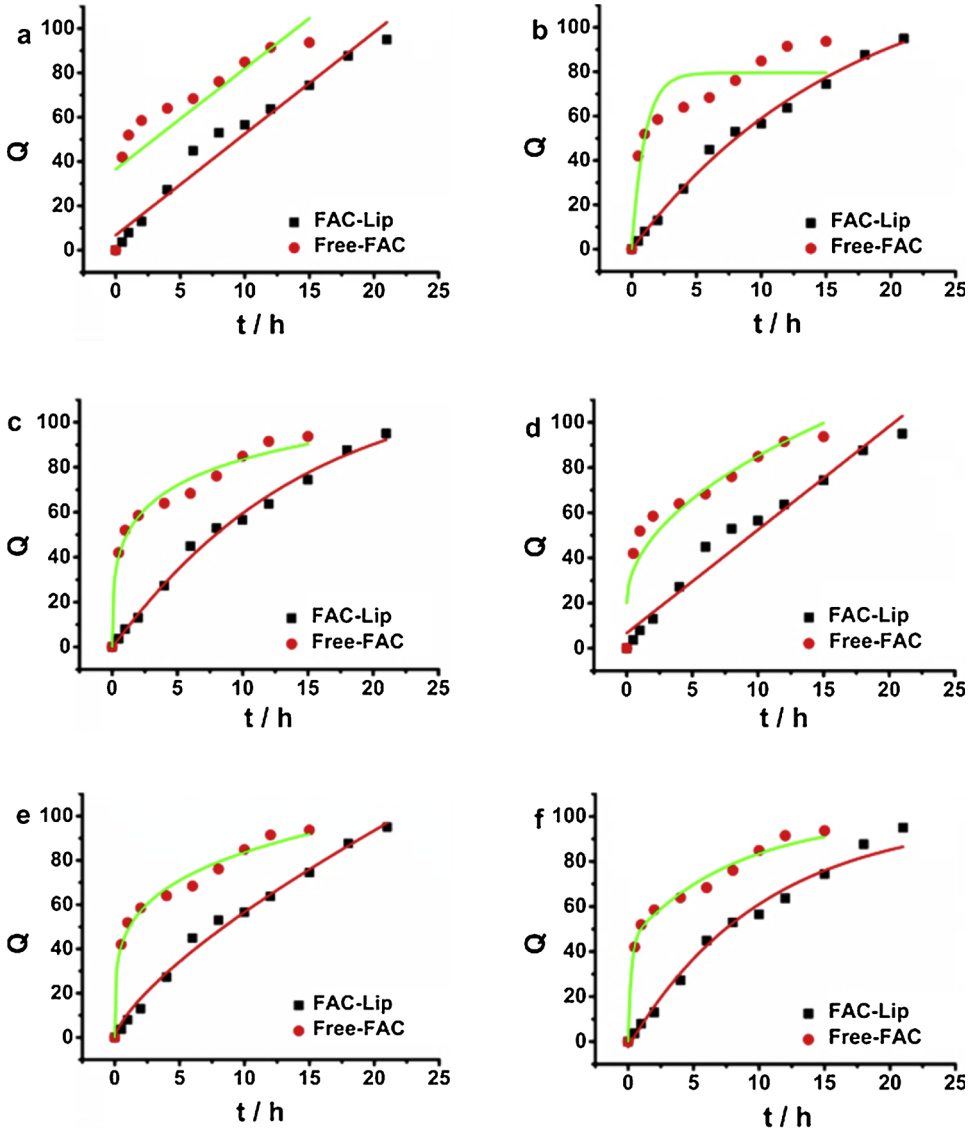

Fig. 5. Release curves of FAC-Lip and free-FAC simulated with Zero order kinetic model (a), First order kinetic model (b), Weibull model (c), Higuchi model (d), Ritger-Peppas model (e), two-phase kinetic model (f) in SIF.

Table 1
Fitted equations by different release models in SGF (Q = cumulative release amount, k = release constant, t = time).

sample	Model	Equation	R^2
FAC-Lip	Zero Order	Q = 0.17612 + 0.00679 t	0.8851
	First order	Q = 0.87873(1-exp(-0.02577 t))	0.9855
	Weibull	Q = 1.04133(1-exp(-(0.01692(t + 0.78756))$^{0.81788}$))	0.9905
	Higuchi	Q = 0.08579 $t^{0.5}$-0.026	0.9879
	Ritger-Peppas	Q = 0.07636$t^{0.5176}$	0.9859
	two-phase	Q = 1-0.20105exp(-0.05481 t)-0.75906exp(-0.01421 t)	0.9955
free-FAC	Zero Order	Q = 0.29593 + 0.04433 t	0.8202
	First order	Q = 0.88235(1-exp(-0.30651 t))	0.8685
	Weibull	Q = 19.06124(1-exp(-(0.08756 (t + 1.72034 × 10^{-8}))$^{0.34551}$))	0.9796
	Higuchi	Q = 0.21299$t^{0.5}$ + 0.1174	0.9599
	Ritger-Peppas	Q = 0.35449$t^{0.33963}$	0.9843
	two-phase	Q = 1-0.28115exp(-5.74853 t)-0.71894exp(-0.13093 t)	0.9813

Table 2
Fitted equations by different release models in SIF (Q = cumulative release amount, k = release constant, t = time).

sample	Model	Equation	R2
FAC-Lip	Zero Order	Q = 0.08448 + 0.0445 t	0.9632
	First order	Q = 1.29643(1-exp(-0.06065 t))	0.9919
	Weibull	Q = 1.93922(1-exp(-(0.02948(t-0.30852))0.81971))	0.9909
	Higuchi	Q = 0.24095t0.5-0.17214	0.9907
	Ritger-Peppas	Q = 0.10685t0.72404	0.9884
	two-phase	Q = 1-9.14806 × 10-4exp(0.23121 t)-1.01253exp (-0.08771 t)	0.9923
free-FAC	Zero Order	Q = 0.36539 + 0.04537 t	0.6978
	First order	Q = 0.79527(1-exp(-0.99182 t))	0.8512
	Weibull	Q = 1.40555(1-exp(-(0.07277(t + 1.6006 × 10-8))0.32819))	0.9725
	Higuchi	Q = 0.20541t0.5 + 0.20152	0.8831
	Ritger-Peppas	Q = 0.48506t0.23631	0.9855
	two-phase	Q = 1-0.44565exp(-4.23224 t)-0.55461exp(-0.12118 t)	0.9849

Table 3
Release mechanisms of FAC-Lip and free-FAC.

media	sample	release exponent (n)	release mechanism
SGF	FAC-Lip	0.5176	non-Fick
	free-FAC	0.3396	Fick
SIF	FAC-Lip	0.7240	non-Fick
	free-FAC	0.2363	Fick

model, and that of free-FAC was 0.9843, which was suitable for Ritger-Peppas model. Table 2 showed that the maximum R^2 of FAC-Lip was 0.9923, so the release of FAC-Lip in SIF was consistent with two-phase kinetic model, and that of free-FAC was 0.9855, which was most consistent with Ritger-Peppas model. The results showed that FAC-Lip accorded with two-phase kinetics model in both SGF and SIF, while free-FAC belonged to Ritger-Peppas model, which showed that the encapsulation of FAC by liposome changed the release model of free FAC.

3.5. Release mechanisms

To study the release mechanisms of FAC-Lip and free-FAC, the release data were fitted with the Ritger-Peppas equation ($Q = k_P t^n$) to calculate n (Table 3). It can be seen that the release mechanisms of FAC-Lip in SGF and SIF belonged to non-Fick diffusion, indicating that the *in vitro*release of FAC-Lip was mainly controlled by the drugs diffusion mechanism. However, the release mechanism of free-FAC in SGF and SIF belonged to Fick diffusion. It suggested that the drug release mechanism would be changed after FAC was encapsulated by liposome.

3.6. The thermal degradation of FAC-Lip

To study the storage stability of FAC-Lip, the effect of temperature on degradation of FAC-Lip was investigated. As shown in Fig. 6 (a) (b), the degradation trends of FAC-Lip and free-FAC were similar. They gradually degraded with the extension of the time. In addition, the degradation gradually increased with the temperature increasing, which may be due to the high temperature accelerating the oxidation or hydrolysis of FAC-Lip, so low temperature was suitable for FAC-Lip storage (Fig. 6a).At the same temperature, the degradation of FAC-Lip was slower than FAC, indicating that encapsulation of the liposomes increased the stability of the FAC. Degradation data were fitted with zero order kinetic model and first order kinetic model, respectively (Table 4). The degradation of FAC-Lip and free-FAC were all consistent with first-order kinetic model. However, the degradation rates of FAC-Lip were slower, indicating that FAC-Lip had a longer shelf life and better stability.

3.7. Thermodynamic parameters analysis

Thermodynamic parameters, such as E_a, ΔH, ΔG, and ΔS, characterizing the degradation processes of FAC-Lip at different temperatures, were calculated according to Eq. (10) – (13) and summarized in Table 5. The data showed that the E_a of FAC-Lip was 26.727 kJ/mol, in the range of 0–50 kJ/mol, which indicated that the degradation of FAC-Lip was less sensitive to temperature. (Wu et al., 2014)

The ΔH represents the energy difference between the reactant and the product, and is related to the strength of the chemical bond of the reactant. The rupture and formation of chemical bond will absorb or release energy during the reaction, which affects the difficulty of reaction. As shown in Table 5, ΔH values were positive at different temperatures, so the degradation of FAC-Lip was an endothermic process, and the smaller ΔH, the more likely degradation. (Blokhina et al., 2016)

The ΔS represents the chaotic change of molecules in the reaction system, and relates to the number of molecules that can actually react. At experiment temperatures, ΔS values were positive, which indicated that the degradation was an entropy-driven process. With temperature increasing, ΔS increased gradually, which indicating that the chaos of

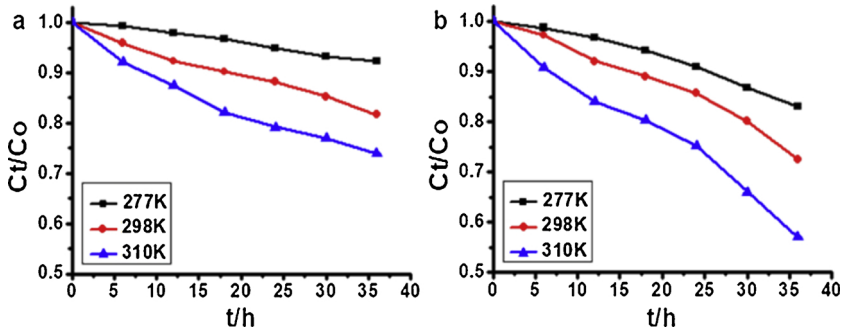

Fig. 6. The degradation curves of FAC-Lip (a) and free-FAC (b) at different temperatures (277 K, 298 K and 310 K).

Table 4
Fitting equations from degradation data of FAC-Lip and free-FAC in PBS (pH 6.5) at 277 K, 298 K and 310 K, respectively.

sample	T (K)	Model	Fitting equation	R2
FAC-Lip	277	First order	ln(Ct/C0) = -0.00161t + 0.00195	0.9917
	298		ln(Ct/C0) = -0.00275t-0.00266	0.9912
	310		ln(Ct/C0) = -0.00593t-0.00357	0.9909
FAC	277	First order	ln(Ct/C0) = -0.00175t + 0.00878	0.9914
	298		ln(Ct/C0) = -0.00292t + 0.00641	0.9909
	310		ln(Ct/C0) = -0.00673t-0.00267	0.9904

Table 5
Thermodynamic parameters of FAC-Lip studied in PBS (pH 6.5) at 277 K, 298 K and 310 K.

sample	T (K)	k	Ea	ΔH	ΔG	ΔS
FAC-Lip	277	0.00161	26.727	24.424	−63.624	297.686
	298	0.00275		24.249	−67.302	307.219
	310	0.00593		24.148	−68.133	317.861

degradation product was higher than that of the reactants, that is, with the temperature increasing, the chaos increased, which intensified the collision between molecules and change the structure of liposome, further accelerated the degradation of FAC-Lip. (Rupar et al., 2018)

In addition, ΔG is the difference between the energy and activation state of a reactant and is often used as a criterion for process spontaneity. In our experiment, the values of ΔG were negative (Table 5), indicating that FAC-Lip degradation was a spontaneous reaction. Moreover, the higher temperature, the faster depredated of FAC-Lip.

4. Conclusions

In this study, FAC-Lip with good sustained-released property was prepared by the rotary-evaporated film-ultrasonic method. FAC-Lip was spherical vesicle, with average size about 178 ± 2.12 nm, negative charge −56 ± 3.51 mV and high encapsulation efficiency 72.77 ± 0.42% (m_{PC}: m_{chol} = 10: 1 and m_{FAC}: m_{PC} = 1: 6.5).

We investigated the *in vitro*release kinetic models and mechanisms of FAC-Lip in SGF and SIF compared with free-FAC. Results showed that the release of FAC-Lip accorded with two-phase kinetic model and non-Fick diffusion, while free-FAC belonged to Ritger-Peppas model and Fick diffusion, which suggested that the encapsulate of FAC by liposome changed the release model and mechanism of free FAC. The store stability of FAC-Lip at different temperatures was also studied and Ea, ΔH, ΔG and ΔS were calculated. Results showed that the degradation of FAC-Lip was an endothermic and spontaneous reaction, and low temperature was suitable for storage.

The results may be helpful in optimizing drug-liposome design, application in food and medicine industries, and furthermore, predicting and guiding medication *in vivo*.

Notes

The authors declare no competing financial interest.

Declaration of Competing Interest

We statement our paper is original and unpublished. It is being submitted only to you and is not being considered for publication at any other journal. We declare no conflict of interest.

Acknowledgments

This research was supported by the National Natural Science Foundation of China (No. 31201305), < GS2 > Natural Science Foundation of Hebei Province < GS2 > (< GN2 > B2019205054 < GN2 >) and Hebei Normal University (L2018Z05), China.

References

Jonker, F.A.M., Boele van Hensbroek, M., 2014. Anaemia, iron deficiency and susceptibility to infections. J. Infect. 69, S23–S27.
Lopez, A., Cacoub, P., Macdougall, I.C., Peyrin-Biroulet, L., 2016. Iron deficiency anaemia. Lancet 387 (10021), 907–916.
Gupta, C., Chawla, P., Arora, S., Tomar, S.K., Singh, A.K., 2015. Iron microencapsulation with blend of gum arabic, maltodextrin and modified starch using modified solvent evaporation method – milk fortification. Food Hydrocoll. 43, 622–628.
Powers, J.M., Buchanan, G.R., 2014. Diagnosis and management of Iron deficiency Anemia. Hematol. Oncol. Clin. North Am. 28 (4), 729–745.
McCullough, P.A., Uhlig, K., Neylan, J.F., Pergola, P.E., Fishbane, S., 2018. Usefulness of oral ferric citrate in patients with iron-deficiency Anemia and chronic kidney disease with or without heart failure. Am. J. Cardiol. 122 (4), 683–688.
Eloy, J.O., Claro de Souza, M., Petrilli, R., Barcellos, J.P.A., Lee, R.J., Marchetti, J.M., 2014. Liposomes as carriers of hydrophilic small molecule drugs: strategies to enhance encapsulation and delivery. Colloids Surf. B Biointerfaces 123, 345–363.
Huang, Y., Hemmer, E., Rosei, F., Vetrone, F., 2016. Multifunctional liposome nanocarriers combining upconverting nanoparticles and anticancer drugs. J. Phys. Chem. B 120 (22), 4992–5001.
Hu, S., Niu, M., Hu, F., Lu, Y., Qi, J., Yin, Z., Wu, W., 2013. Integrity and stability of oral liposomes containing bile salts studied in simulated and ex vivo gastrointestinal media. Int. J. Pharm. 441 (1), 693–700.
Preiss, M.R., Hart, A., Kitchens, C., Bothun, G.D., 2017. Hydrophobic nanoparticles modify the thermal release behavior of liposomes. J. Phys. Chem. B 121 (19), 5040–5047.
Jain, A., Jain, S.K., 2016. In vitro release kinetics model fitting of liposomes: an insight. Chem. Phys. Lipids 201, 28–40.
Yoon, H.Y., Kwak, S.S., Jang, M.H., Kang, M.H., Sung, S.W., Kim, C.H., Kim, S.R., Yeom, D.W., Kang, M.J., Choi, Y.W., 2017. Docetaxel-loaded RIPL peptide (IPLVVPLRRRRRRRRC)-conjugated liposomes: drug release, cytotoxicity, and antitumor efficacy. Int. J. Pharm. 523 (1), 229–237.
Ota, A., Istenič, K., Skrt, M., Šegatin, N., Žnidaršič, N., Kogej, K., Ulrih, N.P., 2018. Encapsulation of pantothenic acid into liposomes and into alginate or alginate–pectin microparticles loaded with liposomes. J. Food Eng. 229, 21–31.
Silva-Weiss, A., Quilaqueo, M., Venegas, O., Ahumada, M., Silva, W., Osorio, F., Giménez, B., 2018. Design of dipalmitoyl lecithin liposomes loaded with quercetin and rutin and their release kinetics from carboxymethyl cellulose edible films. J. Food Eng. 224, 165–173.
Hirai, M., Sato, S., Kimura, R., Hagiwara, Y., Kawai-Hirai, R., Ohta, N., Igarashi, N., Shimizu, N., 2015. Effect of protein-encapsulation on thermal structural stability of liposome composed of Glycosphingolipid/Cholesterol/Phospholipid. J. Phys. Chem. B 119 (8), 3398–3406.
He, Z., Kispert, L.D., Metzger, R.M., Gosztola, D., Wasielewski, M.R., 2000. Carotenoids in liposomes: photodegradation, excited state lifetimes, and energy transfer. J. Phys. Chem. B 104 (26), 6302–6307.
Pérez-Molina, A.I., Juárez-Ordaz, A.J., Gregorio-Jáuregui, K.M., Segura-Ceniceros, E.P., Martínez-Hernández, J.L., Rodríguez-Martínez, J., Ilyina, A., 2011. Thermodynamics of laminarinase partitioning in soya lecithin liposomes and their storage stability. J. Mol. Catal., B Enzym. 72 (1), 65–72.
Niu, Y., Ke, D., Yang, Q., Wang, X., Chen, Z., An, X., Shen, W., 2012. Temperature-dependent stability and DPPH scavenging activity of liposomal curcumin at pH 7.0. Food Chem. 135 (3), 1377–1382.
Wu, C., Xu, X., Feng, C., Shi, Y., Liu, W., Zhu, X., Zhang, J., 2014. Degradation kinetics study of cabozantinib by a novel stability-indicating LC method and identification of its major degradation products by LC/TOF-MS and LC–MS/MS. J. Pharm. Biomed. Anal. 98, 356–363.
Li, N.-N., Geng, L.-N., Wang, L., Yuan, L.-L., Chang, Y.-Z., Zhang, J.-J., 2015. Determination of Iron liposome/water partition coefficients and identification of influencing factors. ActaPhysicoChimicaSinica 31 (11), 2043–2048.
Guo, X., Zheng, H., Guo, Y., Wang, Y., Anderson, G.J., Ci, Y., Yu, P., Geng, L., Chang, Y.-Z., 2017. Nasal delivery of nanoliposome-encapsulated ferric ammonium citrate can increase the iron content of rat brain. J. Nanobiotechnology 15.
Yuan, L., Geng, L., Ge, L., Yu, P., Duan, X., Chen, J., Chang, Y., 2013. Effect of iron liposomes on anemia of inflammation. Int. J. Pharm. 454 (1), 82–89.
Li, N.-N., Geng, L.-N., Wang, L., Li, Y.-Y., Chang, Y.-Z., 2017. Preparation and in vitro release of iron liposome. Journal of Hebei Normal University/NatualScienceEdition 41 (1), 59–64.
Mahobia, S., Bajpai, J., Bajpai, A.K., 2018. Glutaraldehyde crosslinked and alkaline denaturation induced self association of haemoglobin to design nanocarriers for in vitro release of insulin in simulated gastrointestinal fluids (SGFs). J. Drug Deliv. Sci. Technol. 44, 71–81.
Machado, A.R., Pinheiro, A.C., Vicente, A.A., Souza-Soares, L.A., Cerqueira, M.A., 2018. Liposomes loaded with phenolic extracts of Spirulina LEB-18: physicochemical characterization and behavior under simulated gastrointestinal conditions. Food Res. Int.

Gibis, M., Ruedt, C., Weiss, J., 2016. In vitro release of grape-seed polyphenols encapsulated from uncoated and chitosan-coated liposomes. Food Res. Int. 88, 105–113.
Lu, Q., Li, D.-C., Jiang, J.-G., 2011. Preparation of a tea polyphenol nanoliposome system and its physicochemical properties. J. Agric. Food Chem. 59 (24), 13004–13011.
Nayak, A.K., Malakar, J., 2011. Formulation and in vitro evaluation of Hydrodynamically balanced system for theophylline delivery. J. Basic Clin. Pharm. 2 (3), 133–137.
Papadopoulou, V., Kosmidis, K., Vlachou, M., Macheras, P., 2006. On the use of the Weibull function for the discernment of drug release mechanisms. Int. J. Pharm. 309 (1), 44–50.
Siepmann, J., Peppas, N.A., 2001. Modeling of drug release from delivery systems based on hydroxypropyl methylcellulose (HPMC). Adv. Drug Deliv. Rev. 48 (2), 139–157.
Dash, S., Murthy, P.N., Nath, L., Chowdhury, P., 2010. Kinetic modeling on drug release from controlled drug delivery systems. ActaPoloniaePharmaceutica 67 (3), 217–223.
Beltran Osuna, A.A., BoyacaMendivelso, L.A., 2010. Two-phase kinetic model for epoxidation of soybean oil. Ingenieria E Investigacion 30 (2), 188–196.
Koutsoulas, C., Pippa, N., Demetzos, C., Zabka, M., 2014. Preparation of liposomal nanoparticles incorporating terbinafine in vitro drug release studies. J. Nanosci. Nanotechnol. 14 (6), 4529–4533.
Yang, Y., Guo, Y., Tan, X., He, H., Zhang, Y., Yin, T., Xu, H., Tang, X., 2018. Vincristine-loaded liposomes prepared by ion-paring techniques: effect of lipid, pH and antioxidant on chemical stability. Eur. J. Pharm. Sci. 111, 104–112.
Rupar, J., Aleksić, M.M., Nikolić, K., Popović-Nikolić, M.R., 2018. Comparative electrochemical studies of kinetic and thermodynamic parameters of Quinoxaline and Brimonidine redox process. ElectrochimicaActa 271, 220–231.
Limasale, Y.D.P., Tezcaner, A., Özen, C., Keskin, D., Banerjee, S., 2015. Epidermal growth factor receptor-targeted immunoliposomes for delivery of celecoxib to cancer cells. Int. J. Pharm. 479 (2), 364–373.
Soni, V., Kohli, D.V., Jain, S.K., 2008. Transferrin-conjugated liposomal system for improved delivery of 5-fluorouracil to brain. J. Drug Target. 16 (1), 73–78.
Allison, S.A., Xin, Y., Pei, H., 2007. Electrophoresis of spheres with uniform zeta potential in a gel modeled as an effective medium. J. Colloid Interface Sci. 313 (1), 328–337.
Kandzija, N., Khutoryanskiy, V.V., 2017. Delivery of Riboflavin-5′-Monophosphate Into the Cornea: Can Liposomes Provide Any Enhancement Effects? J. Pharm. Sci. 106 (10), 3041–3049.
Shen, H.-L., Yang, S.-P., Hong, L.-W., Lin, L.-Q., Wang, K.-J., Cai, X.-H., Lv, G.-R., 2014. Evaluation of gastric emptying in diabetic gastropathy by an ultrasonic whole stomach cylinder method. Ultrasound Med. Biol. 40 (9), 1998–2003.
Blokhina, S.V., Sharapova, A.V., Ol'khovich, M.V., Volkova, T.V., Perlovich, G.L., 2016. Solubility, lipophilicity and membrane permeability of some fluoroquinolone antimicrobials. Eur. J. Pharm. Sci. 93, 29–37.